Applying the Fractional Generalized Viscoelastic Maxwell Model to Melt Polyethylene Polymer Rheology

Bruno M. Ribeiro Alves [1]

[1]Independent Researcher, Belgium

{Ribeiro Alves,Bruno Manuel} b.bruno.a@gmail.com

Abstract: *This article's goal is to adjust and obtain the adjustment equations for the dynamic SAOS model and its relationship to the property of the polymers. For this, a brief bibliographic review was conducted, and existing data about polymerics' in SAOS were then adjusted. Upon analysis, fitting with Mathematica software it is concluded that the gFMM adjustments are excellent for the observed PE, that the material's adjustment equations were obtained, and that the mechanical properties of flux and flow of materials were then validated. However, it is possible to develop new methodologies based on earlier work and techniques.*

Resumo: *Este artigo tem como objetivo o ajuste e obtenção das equações de ajuste para o módulo dinâmico em SAOS e a sua relação com as propriedades dos polímeros. Para tal fez-se uma breve revisão bibliográfica e em seguida ajustaram-se dados existentes com o software Mathematica sobre materiais poliméricos em SAOS. Conclui-se que os ajustes com o gFMM são excelentes para os PE observados, que se obtiveram as equações de ajuste para o material e consequentemente procedeu-se a validação de propriedades mecânicas de fluxo e de escoamento de materiais. No entanto é de ressalvar que novas metodologias baseadas em trabalhos e técnicas anteriores são formuladas.*

1. Theoretical foundation of work

In this work the objectives are explained, then a brief introduction about rheological models and the behavior and relevance of polymers is done. It will be followed by a new section about the origin of fractional calculus, then by the obtention of the gFMM (generalized fractional Maxwell model) from the cMM (classic Maxwell model). The polymers studied are present part of this paper where the polymers, their relevance towards people, animals and the environment, are studied.

1.1. Objectives of the work

The goals of this paper are to clarify the theory underlying the generalized fractional Maxwell model and Polyethylene, to adjust rheologic dynamic data using the best software currently available the Wolfram Mathematica and to discuss results.

1.2. Rheological Models and the behavior of polymers

1.2.1. Modeling behavior of polymers with simple models

Complex polymer materials, like polyethylene often give rise to counterintuitive phenomena including phenomena of extrudate swell, elastic retraction, Weissenberg effect, and the 1st and 2nd normal stress differences [Bird et al., 1987]. To forecast such complicated actions, a few models like Maxwell classical model or Kelvin-Voigt model have been put out in the literature during the earlier few decades to understand their behavior [Mainardi, 2011].

Table 1: Summary of counterintuitive phenomena of polymers [Bird et al., 1987]

Extrudate swell/ die swell/ Barus effect	This phenomenon occurs when a polymer expands when exiting a die during extrusion, which happens as compressed and aligned polymer chains partially regain their original shape and volume. It is known that the degree of swelling is influenced by the polymer's viscoelasticity, die geometry, and flow rate. It is very important in shaping the final product in industries like blow molding and fiber spinning.
Elastic retraction	This is a phenomenon that refers to the recovery of a material's original shape when the stress or deformation applied to it is removed. This occurs due to the elastic nature of the material, where the internal structure, such as polymer chains in a polymeric substance, strives to return to its relaxed state after being stretched or compressed.
Weissenberg phenomenon	This occurs when a viscoelastic fluid, such as a polymer solution, exhibits an upward climbing behavior along a rotating rod or stirrer, due to the elastic properties of the fluid, causing it to exert normal stresses perpendicular to the flow direction.
1st normal stress difference	The 1st normal stress difference refers to the disparity between the normal stresses in the flow direction and the perpendicular direction in a viscoelastic fluid. This difference arises due to the fluid's elasticity and plays a significant role in understanding its unique behaviors, such as rod climbing (Weissenberg effect) or extrudate swell, in various flow conditions.
2nd normal stress difference	The 2nd normal stress difference is the disparity between the two perpendicular normal stress components in a viscoelastic fluid. It is typically smaller than the 1st normal stress difference and plays a role in understanding flow behaviors like secondary flows and material orientation in complex fluids

1.2.2. Advances in this field regarding viscoelasticity modeling

In the field of viscoelasticity, several researchers are evaluating these theories. For example, Ribeiro Alves, who has published two papers on RCT- Revista de Ciência e Tecnologia related to the use of distinct software to model all traditional and new models [Ribeiro Alves, 2020; Ribeiro Alves, 2022]. These two papers from RCT – Revista de Ciência e Tecnologia demonstrate that it is possible to code with R statistics and to use Excel resulting in good estimation of experimental data [Ribeiro Alves, 2020; Ribeiro Alves, 2022].

However, there are other works that merit to be referred to. As example, a work that investigates the generalization of fractional linear viscoelasticity with the use of variable-order fractional calculus is a pertinent study to consult [Giusti et al., 2024]. Also, there are other works like the use of fractional calculus to predict the viscoelastic responses of materials [Di Paola & Pirrotta, 2022]. A review work of fractional calculus in viscoelastic

models for dynamic solid mechanics problems is another important and recent study [Shitikova, 2022]. And finally, it is mentioned a study that looks at how variable-order fractional operators are used in simulating viscoelastic materials [Yang et al., 2021].

1.2.3. Modeling behavior of polymers with complex models

A model can suit experimental data well or not, in fact it depends on the complexity of data. However, when the complexity of the data is considerable, the simplicity of the model cannot yield, sometimes, exact results. For instance, these models are only applicable to small deformations (cMM – classical Maxwell model and for example cKV – classic Kelvin-Voigt model), or when they cannot forecast typical stress changes. Such models constituted by fractional derivatives and integrals, which have applications in all areas of engineering, have recently more popularity, because of the use of non-integer ordering for derivatives and integrals, which is allowed by these fractional operators, and this can be advantageous when simulating physical processes where memory is crucial, as in the case of viscoelastic fluids.

Since Nutting first proposal of the "spring-dashpot" concept, scientists and researchers had been utilizing and developing fractional calculus [Nutting, 1921]. The spring-dashpot theory is one of the simplest forms and is shown as an unlimited combination of springs and dashpots, and generalized fractional models are typically simply the same models with little or no real relationship to the underlying physics and chemistry. Given that this is a new theory, it is necessary to thoroughly investigate these models to fully understand the theory.

With the spring-dashpot model several classical models were adapted do this theory. The models are the fractional Maxwell model (fMM), which improves on the classical Maxwell model (cMM)by adding fractional derivatives to better capture viscoelastic behavior over a broad range of time scales, is one example of how fractional viscoelastic models are used to describe the behavior of materials with complex time-dependent properties. The fractional Kelvin-Voigt Model (fKV), which describes materials with both elastic and viscous properties, combines fractional calculus with the Kelvin-Voigt model (cKV) [Mainardi, 2011]. Another model has a generalization of the conventional linear solid model, and it is the fractional Zener model, which takes into consideration long-term memory effects in viscoelastic materials by utilizing fractional derivatives [Mainardi, 2011]. Another model is the Scott-Blair model (fSB)which represents power-law creep and relaxation behaviors in viscoelastic solids using fractional calculus [Mainardi, 2011]. Finally, there is the fractional Burgers model (fBM) that describes complex viscoelastic responses, such as creep and stress relaxation, by incorporating fractional derivatives into the classic Burgers model [Mainardi, 2011].

These models can be indeed generalized, such as the fractional generalized Maxwell model (gFMM), which describes complex viscoelastic behavior across a large frequency range by extending the classical Maxwell model (cMM) by adding several fractional elements [Mainardi, 2011]. Comparable to the generalized Maxwell model, the fractional generalized Kelvin-Voigt model (gFKVM) improves on the Kelvin-Voigt model (cKV) by using fractional derivatives to predict viscoelastic qualities more precisely [Mainardi, 2011]. The fractional Poynting-Thomson model (fPT) captures time-dependent viscoelastic responses by combining the Poynting-Thomson model (cPT) with fractional

calculus. Lastly, the fractional Jeffrey Model (fJM) describes both elastic and viscous characteristics in complicated fluids by incorporating fractional derivatives into the Jeffrey model (cJM).

1.3.The fractional derivative model

A fractional derivative is a generalization of a classic derivative that is defined using an integral due to the connection between the two operators required by the calculus fundamental theorem [Padilla, Abreu, and Muma 2008]. The use of fractional derivatives makes various applications in physical modeling processes more visible [Machado, Kyriakova, & Mainardi, 2011]. This operator makes it possible to describe the outcome in a manner distinct from the classical model. We should first describe the theory behind the fractional model before introducing it.

1.3.1. The generalization of fractional calculus theorem

It is known from basic calculus that equation 1 is the first derivative of a determinate function of [Marsden & Weinstein 1985].

$$\frac{\mathrm{d}}{\mathrm{d}x} f(x) \qquad \textbf{Equation 1}$$

It will now be seen how to make this generalization. First it will be recalled the calculus fundamental theorem ["The fundamental theorem of Calculus" 2010].

***Theorem* 1**(Calculus Fundamental Theorem):
$If f: [a, b] \to \mathbb{R}$ a continuous function, and if
$F: [a, b] \to \mathbb{R}$ defined by

$$F(x) \coloneqq \int_a^x f(t)\, dt$$

So, F is differenciable and:

$$\frac{d}{dx} F = f$$

So, these two operators are linked, as announced by this theorem. The Riemann's integral operator will be presented in the following section.

***Case*1**: $If f is$ an integrable function on Riemann on interval [a,b]. So, for $x \in$ [a,b] and n $\in \mathbb{N}$,we have

$$\underbrace{\int_a^x \int_a^x \dots \int_a^x f(x)dxdx\dots dx}_{ntimes} = J_a^n f(x) = \frac{1}{(n-1)!}\int_a^x (x-t)^{n-1} f(t)dt$$

Because it enables the use of operator for values n that are not natural numbers, this notation is incredibly helpful. The only issue is that the formula contains a factorial that prevents this quick generalization, making the Euler function necessary for the answer to emerge [Freed, Diethelm, & Luchko, 2002]. The Gamma of Euler function will now be presented.

$Definition1$: Function Γ: (0,∞) → ℝ,defined by

$$\Gamma(x) := \int_0^{\infty} t^{x-1}\, e^{-t} dt,$$

has the name of Gamma of Euler

This function generalizes the factorial for n values integers (theorem 2):

$Theorem2: For\ n \in \mathbb{N}$ we have that$(n-1)!$ =$\Gamma(n)$

We are now in the condition to obtain the generalized integral:

$Definition2$: If $n \in \mathbb{R}_+$. Fractional Integral of **Riemann − Liouville** of order n is defined by:

$$J_a^n f(x) = \frac{1}{\Gamma(n)} \int_a^x (x-t)^{n-1} f(t) dt$$

For $x \in$ [a,b]e J_a^ndefined on the space L_1[a,b].

Next, we will obtain the generalized derivative:

$Definition$ 3: If $n \in \mathbb{R}_+$ and $m = \lceil n \rceil$. The operator D_a^ndefined by:

$$D_a^n f = \underbrace{\frac{d}{dx}\frac{d}{dx}\ldots\frac{d}{dx} f(x) dx dx \ldots dx}_{ntimes} := D^m J_a^{m-n}$$

is called of fractional derivative of Riemann-Liouville of order n

Another way to write the derivative is:

$Definition$ 4: If $\alpha \in \mathbb{R}_+$ and $m = \lceil \alpha \rceil$. The operator $D_a^{\alpha} defined$ by:

$$D_a^{\alpha} f = \frac{1}{\Gamma(n-\alpha)} \frac{d^m}{dt^m} \int_a^x (x-t)^{-\alpha+m-1} f(t) dt$$

is called fractional derivative of Riemann-Liouville of order $m-1 < \alpha < m$.

However, by using the definition of Riemann-Liouville it is still difficult to impose border conditions.

So, it is seen calculating the Laplace transform of fractional derivative $D_0^{\alpha} f$, which is given by:

$$L\{D_0^{\alpha} f(t)\} = s^n F(s) - \sum_{k=0}^{n-1} s^k [D_0^{\alpha-k-1} f(t)]_{t=0}$$

What means that we must know the value of fractional derivative at point zero.

The solution to this problem is given by Caputo, as seen on definition 5:

$Definition$ 5: $If\ n > 0\ and\ m = \lceil n \rceil$. We define the operator $\widehat{D}_a^n$:
$\widehat{D}_a^n f := J_a^{m-n} D^m f$
always that $D^m f \in L_1$[a,b].

The Caputo operator is now written in the following way:

$Theorem$ 3: $If\ n > 0 and\ m = \lceil n \rceil. we$ assume that $f \in A^m[a,b]. So$:
$\widehat{D}_a^n f := D_a^n [f - T_{m-1}[f,a]]$
$T_{m-1}[f,a] is$ the Taylor polinomium of degree $m-1 for$ f function,centered in a:

$$T_{m-1}[f,a](x) = \sum_{k=0}^{m-1} \frac{f^{(k)}(a)}{k!}(x-a)^k$$

Having consideration, the theorem three the Caputo operator has a new format:

$Definition$ **6**: If $n > 0$e, we assume that $D_a^n\left[f - T_{m-1}[f,a]\right]$ exist, with $m = \lceil n \rceil$. So, we define the operator D_{*a}^n:
$D_{*a}^n f := D_a^n\left[f - T_{m-1}[f,a]\right]$
$D_{*a}^n f$ *have* name of Caputo differential operator of order n..

This definition is finally written by:

$Definition$ **7**: If $\alpha \in \mathbb{R}_+$ and $m = \lceil \alpha \rceil$. The operator $D_a^n defined$ by:
$$D_{*a}^{\alpha} f = \frac{1}{\Gamma(m-\alpha)} \int_a^x (x-t)^{-\alpha+m-1} \frac{d^m f(t)}{dt^m} dt$$
is called Caputo Fractional Derivative of order $m-1 < \alpha < m$.

The Laplace transform of derivative $D_{*0}^{\alpha} f$ is given:

$$L\{D_{*0}^{\alpha} f(t)\} = s^n F(s) - \sum_{k=0}^{n-1} s^k [f^{(k)}(0)]$$

.

Which for this new definition of Caputo Fractional Derivative if f is a speed f' will represent an acceleration. In this way Caputo fractional derivative is used on resolution of physics problems.

1.3.2. From cMM (classic Maxwell model) to gFMM (generalized Fractional Maxwell model)

It is known that the Maxwell classic model relaxation shows an exponential decline, it is possible to draw a relationship between the gFMM and the cMM [Macosko 1994]. cMM relaxation modulus is seen on equation 2, where G(t) is the relaxation modulus in function of time, G0 the initial relaxation modulus value, t the value of time and e corresponding to the exponential function and finally λ the value of relaxation time.

$$G(t) = G_0 e^{-t/\lambda} \qquad \textbf{Equation 2}$$

Its constitutive equation results on the integral model as presented on equation 3, where τ (t) is the constitutive integral equation of Maxwell model, G0, the initial value relaxation modulus, t is the corresponding time at instant t1 and t' the values of time at an instant t2 and finally $\dot{\gamma}$ as the deformation rate [Bird, Armstrong, and Hassanger 1987]

$$\tau(t) = -\int_{-\infty}^{t} G_0 e^{-(t-t')/\lambda} \dot{\gamma}(t') dt'. \qquad \textbf{Equation 3}$$

But what really happens is that neither all materials presents this type of behavior, being the most common the algebraic decay given by equation 4, where A is a quasi-property dependent and fractional order α at a time t [Jaishankar & McKinley, 2012]:

$$G(t) = \frac{A}{\Gamma(1-\alpha)} t^{-\alpha} \quad \textbf{Equation 4}$$

The resultant model is given by equation 5.

$$\tau(t) = \int_{-\infty}^{t} \frac{A}{\Gamma(1-\alpha)} (t-t')^{-\alpha} \dot{\gamma}(t') dt' = \frac{A}{\Gamma(1-\alpha)} \int_{-\infty}^{t} (t-t')^{-\alpha} \dot{\gamma}(t') dt' \quad \textbf{Equation 5}$$

Remembering the definition of Caputo fractional derivative, it can be assumed that to perform modeling from t = a it is obtained the following expression for tension, as presented below on equation 6.

$$\tau(t) = AD^{\alpha}_{*a}\gamma(t) = A\frac{d^{\alpha}\gamma(t)}{dt^{\alpha}} \quad \textbf{Equation 6}$$

cMM is obtained from a combination of a Spring and a dashpot, but gFMM is obtained from a combination of two springpot.

Indeed, gFMM constitutive equation is obtained throughout the addition of total deformations imposed in the presence of each springpot (see equation 7), where Φ1 corresponds to a quasi-property related to fractional order α, and Φ2 a quasi-property related to fractional order β [Jaishankar and McKinley 2012],

$$\tau + \frac{\Phi_1}{\Phi_2} \frac{d^{\alpha-\beta}\tau}{d^{\alpha-\beta}t} = \Phi_1 \frac{d^{\alpha}\gamma(t)}{dt^{\alpha}} \quad \textbf{Equation 7}$$

It is expected for the equation 7 full derivation without loss of generality. As a result, MFM has four parameters: the fractional orders and the quasi-properties). [Jayshankar and McKinley 2012]

For the Maxwell Generalized Fractional Model on a stress-relaxation experiment, is possible to have equation 8, where γ_0 is the initial value of deformation:

$$G(t) = \frac{\tau(t)}{\gamma_0} \quad \textbf{Equation 8}$$

Which results on equation 9:

$$G(t) = \Phi_2 t^{-\beta} E_{\alpha-\beta,1-\beta}\left(-\frac{\Phi_2}{\Phi_1} t^{\alpha-\beta}\right) \quad \textbf{Equation 9}$$

Where $E_{a,b}(z)$ is the Mittag-Leffler function (equation 10):

$$E_{a,b}(z)=\sum_{k=0}^{\infty}\frac{z^k}{\Gamma(ak+b)} \qquad \textbf{Equation 10}$$

On creep experiments, defined by J(t), for Maxwell generalized fractional model we have equation 11, where J(t) is the compliance creep modulus and γ(t) deformation in function of time and τ_0 the initial value of stress:

$$J(t)=\frac{\gamma(t)}{\tau_0} \qquad \textbf{Equation 11}$$

Which results on equation 12:

$$J(t)=\frac{1}{\Phi_1}\frac{t^{\alpha}}{\Gamma(1+\alpha)}+\frac{1}{\Phi_2}\frac{t^{\beta}}{\Gamma(1+\beta)} \qquad \textbf{Equation 12}$$

It is evaluated the complex modulus using the procedure of Friederich [Friedrich 1991] and Schiessel [Schiessel, Metzler, Blumen, & Nonnenmacher, 1995] and the constitutive equation is at equation 13 [Jaishankar and McKinley 2012)

$$\tau+\frac{\Phi_1}{\Phi_2}\frac{d^{\alpha-\beta}\tau}{d^{\alpha-\beta}t}=\Phi_1\frac{d^{\alpha}\gamma(t)}{dt^{\alpha}} \qquad \textbf{Equation 13}$$

Plus, the Fourier transform of Caputo derivative is at equation 14.

$$\tau\left\{\frac{d^{\alpha}}{dt^{\alpha}}f(t);\omega\right\}=(i\omega)^{\alpha}\,\tilde{f}(\omega) \qquad \textbf{Equation 14}$$

To obtain the complex modulus G* (ω) where an imaginary number is presented (equation 15):

$$G^*(\omega)=\frac{\Phi_1(i\omega)^{\alpha}\Phi_2(i\omega)^{\beta}}{\Phi_2(i\omega)^{\alpha}\Phi_1(i\omega)^{\beta}} \qquad \textbf{Equation 15}$$

Evaluating the real part and the imaginary part it is possible to have equation 16 for the storage modulus G'(ω) and equation 17 for the loss modulus G''(ω), where cos is related to cosine and sin to sinus:

$$G'(\omega)=\frac{(\Phi_2\omega^{\beta})^2\Phi_1\omega^{\alpha}Cos\left(\frac{\pi}{2}\alpha\right)+(\Phi_1\omega^{\alpha})^2\Phi_2\omega^{\beta}Cos\left(\frac{\pi}{2}\beta\right)}{(\Phi_1\omega^{\alpha})^2+(\Phi_2\omega^{\beta})^2+2\Phi_1\omega^{\alpha}\Phi_2\omega^{\beta}Cos\left(\frac{\pi}{2}(\alpha-\beta)\right)} \qquad \textbf{Equation 16}$$

$$G''(\omega) = \frac{(\Phi_2\omega^{\beta})^2\Phi_1\omega^{\alpha}Sin\left(\frac{\pi}{2}\alpha\right) + (\Phi_1\omega^{\alpha})^2\Phi_2\omega^{\beta}Sin\left(\frac{\pi}{2}\beta\right)}{(\Phi_1\omega^{\alpha})^2 + (\Phi_2\omega^{\beta})^2 + 2\Phi_1\omega^{\alpha}\Phi_2\omega^{\beta}Cos\left(\frac{\pi}{2}(\alpha-\beta)\right)} \qquad \textbf{Equation 17}$$

2. Polymers studied

In this paper, three primary types of polymers are used. While a polymer corresponds to a polymer made using EXXPOL ® catalyst technology (Exxon Mobil Exact 0201), a metallocene catalytic reaction, there is a first one corresponding to LDPE (Low Density Polyethylene) and catalyzed by free radical polymerization with the commercial name Equistar Petrothene NA 952-00. The last polymer is an LLDPE produced using Ziegler-Natta catalysis under the commercial name Exxon Mobil NTX 101.

2.1. Equistar Petrothene NA 952-00

According to LyondellBasell (2025), this polymeric resin is used in blow molding [Doerpinghaus, 2002], packaging (blow molding-bag applications), injection molding, and linear applications. Additionally, this commercial resin is made with peroxide catalysts in a high-pressure autoclave [Doerpinghaus, 2002] and has good softness, good toughness, and good dimensional stability [LyondellBasell, 2025]. The polymerization reaction begins with the cleavage of the O-O peroxide bond and continues until it is halted by an "operator's hand" or the reagent running out [Vasile and Pascu, 2005]. As seen in figure 1, we begin with an unstable peroxide that can split into two peroxide radicals.

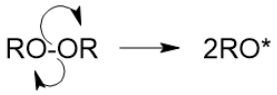

Figure 1: Reaction of an unstable peroxide to form two peroxide radicals.

The extremely unstable peroxide radical will then react with an ethylene molecule. The radical will dislocate to the molecule's last carbon atom because of the reaction between the radical and the ethylene molecule's double connection. As seen in figure 1, this is the first stage of radical polymerization.

Figure 2: Initiation step of radical polymerization of polyethylene

The propagation process comes next, in which n ethylene molecules will react with the molecules shown in figure 1 (refer to figure 3).

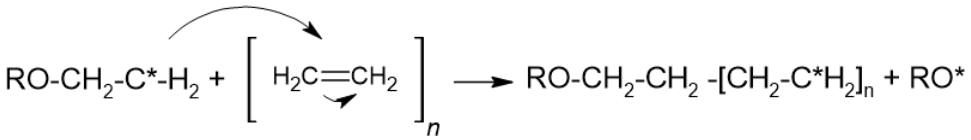

Figure 3: Propagation step of radical polymerization of polyethylene

The polymerization's termination reaction can be seen as the amount of ethylene gets closer to its limit. The termination can occur between the initial radical, between the polymeric chain's parts, causing branching, or even between hydrogen donors that the employee mixes (see figure 4).

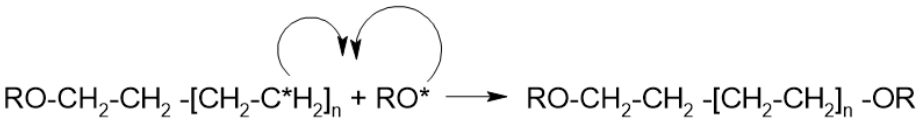

Figure 4: Example of termination step of radical polymerization of polyethylene with peroxide radical

2.1.1. Relevance of Equistar Petrothene NA 952-00

Low-density polyethylene (LDPE) resin Equistar Petrothene NA 952-00 is frequently utilized in blow molding, injection molding, and packaging. It is renowned for having outstanding dimensional stability, softness, and toughness. Because it strikes a compromise between processability and durability, this material is frequently chosen for items including caps, closures, squeeze bottles, and liners [LyondellBasell, 2025]. Low-density polyethylene (LDPE) Equistar Petrothene NA 952-00 affects humans, animals, and the environment in several ways [LyondellBasell, 2025].

Its uses for people include making everyday life easier through its widespread use in consumer items including bottles, caps, and packaging [LyondellBasell, 2025]. The resin's safety in food packaging applications is guaranteed by its compliance with FDA food contact requirements [LyondellBasell, 2025]. It has an indirect effect on animals because, although LDPE products are not directly toxic to animals, incorrect disposal might result in ingestion or entanglement, which could endanger wildlife. It is non-biodegradable for the environment because, like most plastics, LDPE does not biodegrade and, if improperly handled, can contribute to long-term environmental damage. This material is recyclable, has varying recycling rates, and can accumulate in landfills and the ocean if improperly disposed of.

2.2. Exxon Mobil NTX 101

Exxon Mobil NTX 101 is the initiator of a Ziegler-Natta polymerization reaction that the polymer goes through [Vasile and Pascu 2005]. As can be seen below a simplest reaction

design, the polymerization reaction goes through three stages: initiation (figure 5), propagation (figure 6), and termination (figure 7).

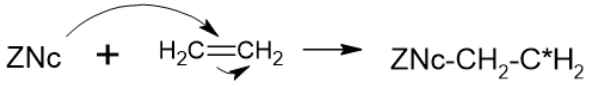

Figure 5: Initiation step of Ziegler Natta catalytic (ZNc) polymerization of polyethylene

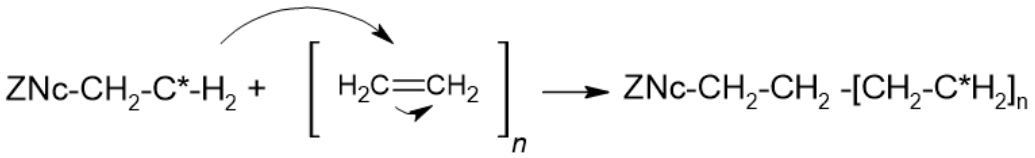

Figure 6: Propagation step of Ziegler Natta catalytic (ZNc) polymerization of polyethylene

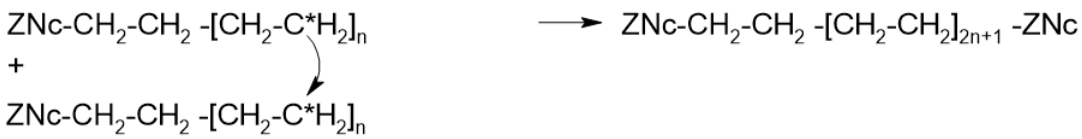

Figure 7: Example of the typical termination step of Ziegler Natta catalytic (ZNc) polymerization of polyethylene

2.2.1. Relevance of Exxon Mobil NTX 101

The linear low-density polyethylene (LLDPE) resin ExxonMobil NTX 101 is renowned for its super strength and toughness properties, especially about resistance to impact and tearing [Exxon Mobil NTX 101, 2025]. It is pertinent in several areas: for individuals it offers flexibility and durability when used in blown stretch films, which makes it perfect for industrial and packaging applications [Exxon Mobil NTX 101, 2025]. For safety it has consistent performance and is ensured by its stabilization for extrusion processes and lack of antiblock or slide additives [Exxon Mobil NTX 101, 2025].

Like other plastics, improper disposal can lead to environmental pollution, which may harm wildlife through ingestion or entanglement. While it is recyclable, its environmental impact depends on proper waste management practices. As a plastic resin, it contributes to long-term pollution if not handled responsibly.

2.3. Exxon Mobil Exact 0201

Exxon Mobil EXACT 0201 is an ethylene octene copolymer made with ExxonMobil Chemical's EXXPOL™ Technology. According to Ethylene-based Plastomer Resin (2012), it is designed for use in blown film applications that need outstanding durability and sealability in both monolayer and multilayer configurations.

The basic scheme of polymerization is shown in Figure 8 for the initiation stage, Figure 9 for the propagation step, and Figure 10 for the termination step of polyethylene, as is also the case with other polyethylene's.

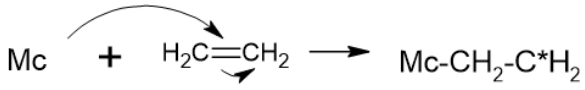

Figure 8: Initiation step of Metallocene catalytic (Mc) polymerization of polyethylene

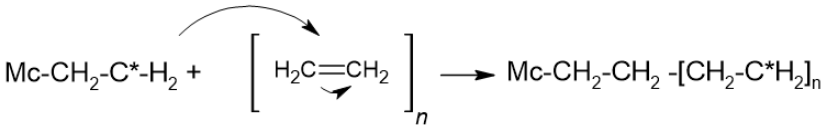

Figure 9: Propagation step of Metallocene catalytic (Mc) polymerization of polyethylene

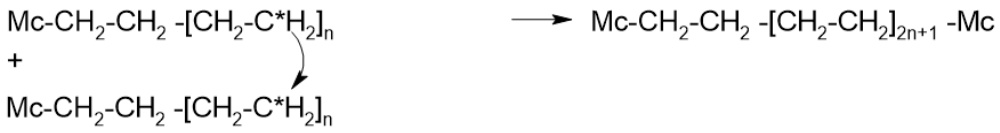

Figure 9: Termination step of Metallocene catalytic (Mc) polymerization of polyethylene

2.3.1. Relevance of Exxon Mobil Exact 0201

ExxonMobil Exact 0201 is a Plastomer resin based on ethylene that has special qualities that make it ideal for several uses: it is perfect for industrial blown film applications because of its exceptional impact strength and sealability, guarantees easy handling and processing in lamination and packaging and has high clarity because of superior optical qualities for applications involving transparent films [ExxonMobil Exact 0201, 2012]. It also performs well in sealing applications at lower temperatures thanks to its low temperature Sealability [ExxonMobil Exact 0201, 2012]. It is applied to industrial and food packaging in both monolayer and multilayer films, is ideal for uses that call for durability and high adherence and is perfect for goods that need to be flexible and durable [ExxonMobil Exact 0201, 2012]. Like other polymers, it harms the environment.

3. Fractional models in polymerization and environment

Numerous environmental consequences, including polymer synthesis and environmental systems, can be linked to the fractional model.

3.1.Fractional Models in Polymer Synthesis

The rheological behavior of polymer systems is described by the gFMM. These models are known to work best for materials that behave power-law, like solutions of entangled polymers. The viscoelastic properties of polymers, which are essential for applications like coatings and biomedical devices, can be revealed by the gFMM with fewer parameters than the cMM [Schmidt et al., 2024]

3.1.Environmental Impact of Polymer Synthesis

Traditional techniques of polymer production require petrochemicals, which contribute to waste and pollution. To cut down on plastic waste and promote a circular economy, green polymer synthesis, biodegradable polymers like PLA and PHA, and recycling technologies provide more environmentally friendly options [Beena Unni & Muringayil Joseph, 2024].

In environmental research, fractional models are effective instruments that provide a sophisticated method of comprehending intricate systems, such as the dispersion of pollutants, the control of water pollution, and complex occurrences [Beena Unni & Muringayil Joseph, 2024]. To simulate the spread of contaminants in heterogeneous media, fractional models are used, such as those that use Mittag-Leffler functions. To properly forecast pollutant dynamics, these models must account for memory effects and nonlocal interactions [Beena Unni & Muringayil Joseph, 2024]. So fractional models are more and more interesting in these domains because researchers can have another look into the systems.

So, researchers can more thoroughly examine the dynamics of water pollution transmission by including fractional calculus into modeling frameworks. This entails determining equilibrium points and putting the best management measures in place to lessen pollutants [Beena Unni & Muringayil Joseph, 2024].

Processes like anomalous diffusion and subterranean water filtration are studied using fractional models. They are perfect for simulating complex environmental processes because they can take nonlocality and energy dissipation into account [Beena Unni & Muringayil Joseph, 2024].

4. Methodology

The methodology used in this work was an exploratory analysis of data using for that the software Mathematica. For this analysis three different types of commercial polyethylene resins, which include Exxon Mobil NTX 101, Equistar Petrothene NA 952-00, and Exxon Mobil Exact 0201 commercial resins will have data collected from literature. The data is from dynamic experimentation in SAOS and comes from Doerpinghaus study [Doerpinghaus, 2002]. The Rheometric Mechanical Spectrometer Model 800 (RMS 800) was the instrument used to perform the torsional rheometric test. [2002, Doerpinghaus]. Doerpinghaus used cone-plate test rigs with a 25 mm diameter and a cone at an angle of 0.1 radians to test all polymeric materials at 170°C in an inert nitrogen atmosphere [Doerpinghaus, 2002].

Upon code construction, the adjustments are done in the same graphic as the Maxwell fractional model, and it is performed two times to calculate the relative error of the measure. The code of Normand et al is very useful because it can be adapted for a large number of situations, as Alves, have done in 2017 research, which was published in the King Saud University Journal of Engineering Sciences [Alves, 2017].

Alves, by modifying Normand's source code [Normand, Eisenberg, & Peleg, 2012] to perform fractional viscoelastic adjustments of metallocene-catalyzed polyethylene using the commercial program Wolfram Mathematica, demonstrated a novel method for carrying out adjustments of fractional viscoelastic equations [Alves, 2017].

The enhancements now were actualized to the capacity to introduce more than three different types of data and more than four datasets, each of which contains the required number of equations for material functions. With this recent modification, it is now possible to produce brand-new, high-resolution images without the need for Photoshop or even a lot of paint. It's easier because there's less code now. Several changes must be made to CDF files. However, a limitation exists regarding the number of equations that it is possible to adjust.

Three datasets, each containing data corresponding to G'(ω), G"(ω), and G"(ω)/G'(ω), three fractional equations (storage modulus, loss modulus, and phase angle of gFMM), and a fit button are all included in the software's cdf code. Compared to Alves' code [Alves, 2017], this is better because Alves required a new CDF code for every material.

4. Results

4.1. Equistar Petrothene NA 952-00

Examining each experimental match for the polymer Equistar Petrothene NA 952-00 with the SAOS material functions for the Maxwell fractional model, it appears to fully comply with the requirements of thermodynamics. As a result, each adjustment's R^2 adjustment is faultless and at an high level. Also, the relative error for the second experimental fit can be seen to be extremely low for all parameters. This can be analyzed on table 2.

Table 2 - Results for two different adjustments for FMM model for polymer Equistar Petrothene NA 952-00 in logarithmic scale in SAOS experiments and the correspondent relative error (%)

First fit Experiment					
Parameters	α	β	Φ_1	Φ_2	R^2
G'(ω)	0.82	0.366000	12230	11030	1.00000
G'' (ω)					
G''(ω)/ G'(ω)					
Second fit experiment					
Parameters	α	β	Φ_1	Φ_2	R^2
G'(ω)	0.825077	0.366421	12232.19	11026.79	0.99999
G''(ω)					
G''(ω)/ G'(ω)					
Relative error					
	α	β	Φ_1	Φ_2	
1st and 2nd adjustment	0.00933 %	0.1150 %	0.0179 %	0.0291 %	

Figure 10 presents the modification of the polymer Equistar Petrothene NA 952-00 with respect to the Maxwell fractional model's material functions. Storage modulus fit

(blue line), loss modulus fit (orange line), and phase angle fit (green line) are all perfectly adjusted to, or coincide perfectly, with, experimental data. The adjustment in this case is for the initial experimental fit to achieve the best fit outcomes. This image (figure 10) is a case study of the mean values of the two fit parameters.

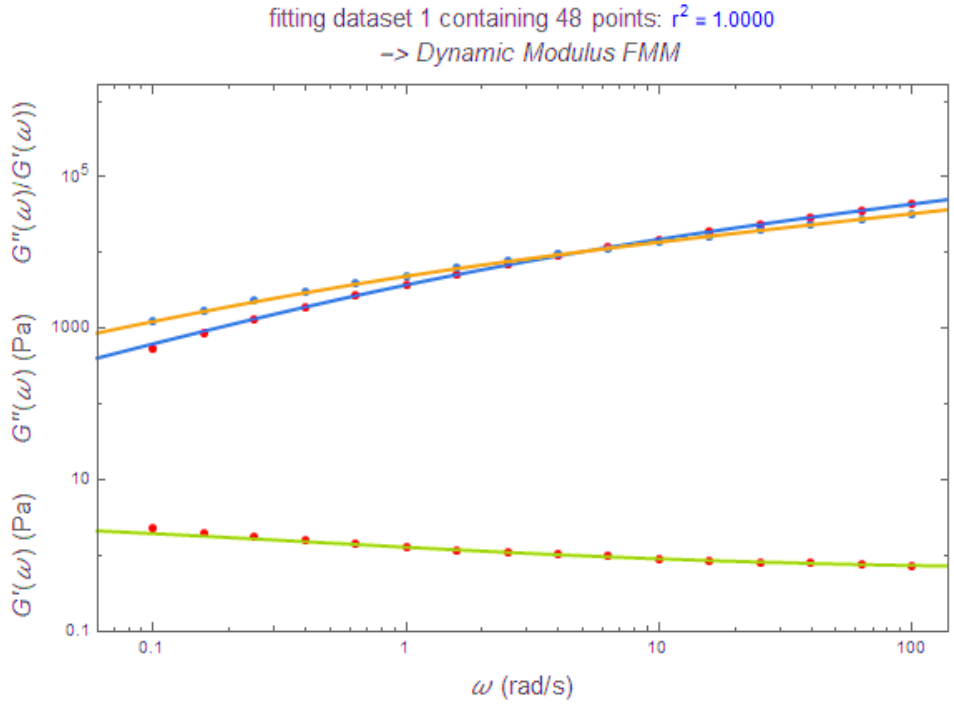

Figure 10: First experimental adjustment with software Mathematica for polymer Equistar Petrothene NA 952-00 with Maxwell fractional model in SAOS experiments.

4.2. Exxon Mobil NTX 101

For Exxon Mobil NTX 101 polymer's parameter values for the Maxwell fractional model comply with the thermodynamic criteria. For each fit modification, the resulting R^2 adjustment is quite high and flawless. Table 3 shows that for all parameters, the relative error is extremely low.

Table 3 - Results for 2 different adjustments for FMM model for polymer Exxon Mobil NTX 101 in logarithmic scale in SAOS experiments and the correspondent relative error (%)

First fit Experiment					
Parameters	α	β	Φ_1	Φ_2	R^2
G'(ω)	0.92600	0.37700	51730	12010	1.00000
G''(ω)					
G''(ω)/ G'(ω)					
Second fit experiment					

Parameters	α	β	Φ_1	Φ_2	R^2
G' (ω)	0.926468	0.377087	51732.25	12007.98	0.99999
G'' (ω)					
G''(ω) / G'(ω)					
Relative error					
	α	β	Φ_1	Φ_2	
1st and 2nd adjustment	0.0505 %	0.02308%	0.004349 %	0.0168%	

The modification of the polymer Exxon Mobil NTX 101 with material functions of the Maxwell fractional model is shown in Figure 2. Storage modulus fit (blue line), loss modulus fit (orange line fit), and phase angle fit (green line fit) are all perfectly adjusted to or coincide perfectly with experimental data. The adjustment shown here is for the first experimental adjustment since there are superior results for the first experimental fit. As can be seen, however, the quality of adjustment is worse for values of less than 1 rad/s where there is a little discrepancy between the adjusted models of storage modulus (blue line) and phase angle (green line) and the corresponding experimental sites.

A perfectly legitimate thermodynamic requirement exists. As a result, each adjustment has an extremely high and flawless R^2 adjustability. Considering this, the relative error is small.

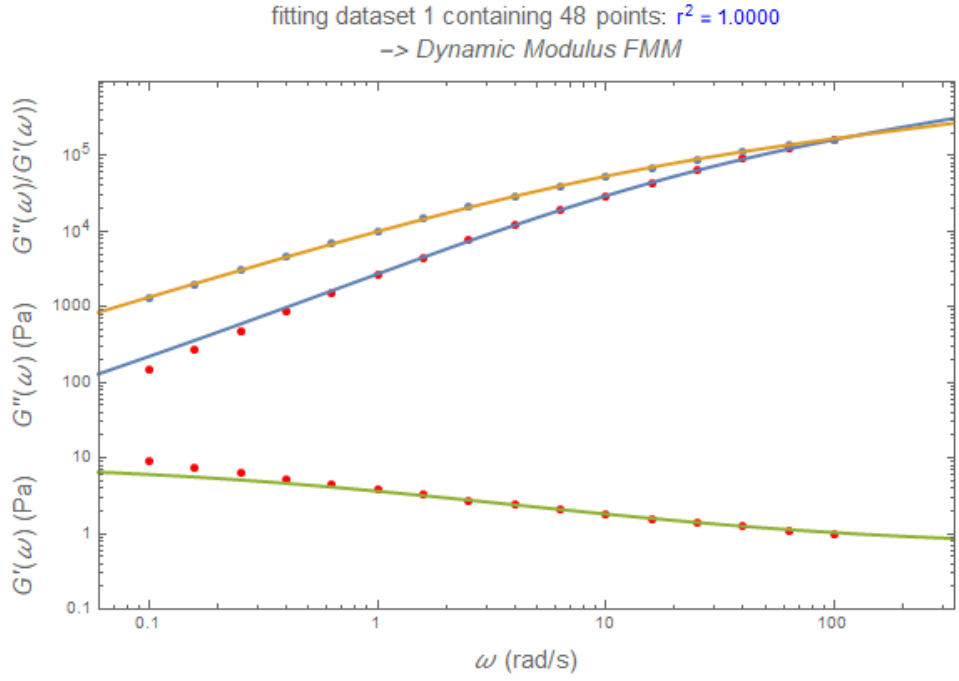

Figure 12: First experimental adjustment with software Mathematica for polymer Exxon Mobil NTX 101 with Maxwell fractional model in SAOS experiments

4.3. Exxon Mobil Exact 0201

Finally, table 4, presents the results for two adjustments for gFMM for polymer Exxon Mobil Exact 0201 in logarithmic scale in SAOS dynamic experiments. It is seen high correlation levels between the first and the second adjustments and the models obeys to thermodynamics restrictions imposed.

Table 4 - Results for two different adjustments for FMM model for polymer Exxon Mobil Exact 0201 in logarithmic scale in SAOS experiments and the correspondent relative error (%).

First fit Experiment					
Parameters	α	β	Φ_1	Φ_2	R^2
G'(ω)	0.75200	0.353000	11760	74040	1.00000
G''(ω)					
G''(ω)/ G'(ω)					
Second fit experiment					
Parameters	α	β	Φ_1	Φ_2	R^2
G'(ω)	0.75200	0.353318	11758.8	74035.23	0.9999857
G''(ω)					
G''(ω)/ G'(ω)					
Relative error					
	α	β	Φ_1	Φ_2	
1st and 2nd adjustment	0 %	0.09008 %	0.0102%	0.00644%	

The adjustment of the polymer Exxon Mobil Exact 0201 with material functions of the Maxwell fractional model is shown in Figure 13. Storage modulus fit (blue line), loss modulus fit (orange line fit), and phase angle fit (green line fit) are all perfectly in line with the experimental data. Because there are superior results for first experimental fit, the adjustment is for first experimental fit as shown above.

However, as can be seen in Figure 12, the quality of adjustment is worse for values below 0.4 rad/s, where there is a little discrepancy between the experimental storage modulus and phase angle points and the adjusted model's blue and green lines, respectively.

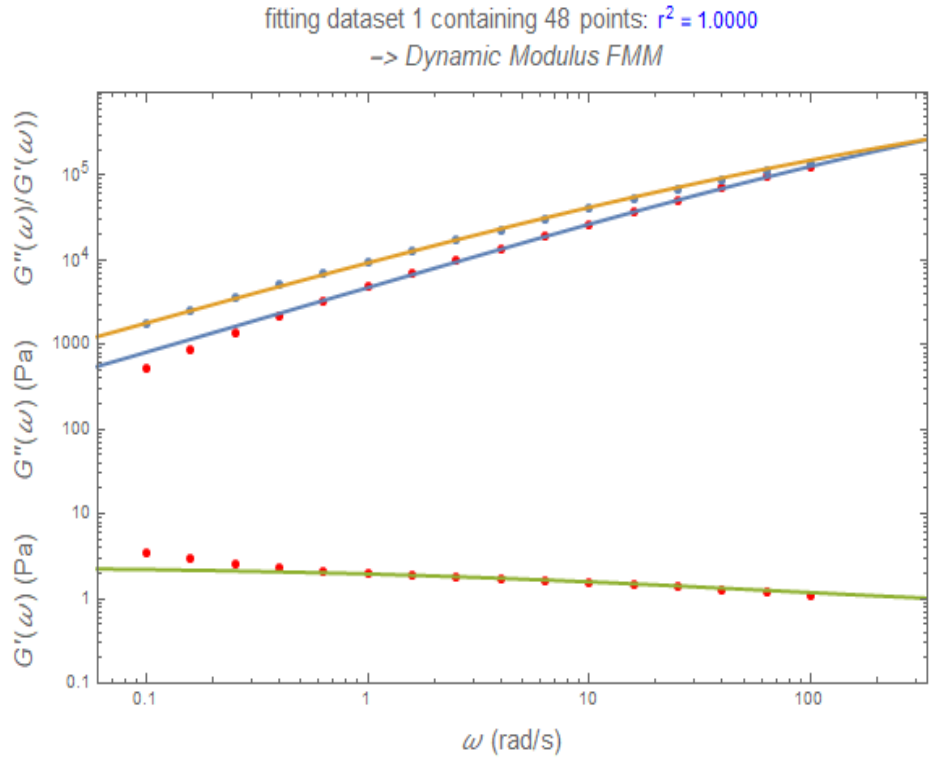

Figure 13: First experimental adjustment with software Mathematica for polymer Exxon Mobil Exact 0201 with Maxwell fractional model in SAOS experiments

5. Discussion of results

The first finding from the results is that all the parameters have the same order of magnitude. The model can predict properties like density, the melt flow index, the long chain branching, the molecular weight, and the polydispersity index of all the commercial resins evaluated since the adjustments are perfect for the Maxwell fractional model.

Therefore, this study predicts the behavior of three polymers, Equistar Petrothene NA 952-00, Exxon Mobil NTX 101 G'(ω), and Exxon Mobil Exact 0201, in torsional rheometer (SAOS) at the intervals shown in Table 14:

Table 4: Intervals confirmed because of the perfect adjustment observed with Maxwell fractional model in SAOS experiments.

Parameter	Value
Density (g/cm^3)	0.902-0.919
Melt flow index	0.9-1.1
Long Chain branching	0.79 – 39
Mw	88700 – 235500
Mw/Mn (Polydispersity index)	2.14 – 17.1

On table 5 the predictions were resumed.

Table 5: Specific characteristics validated for each polymer [Doerpinghaus, 2002]

Molecular weight and polymerization degree	Each PE has specific molecular weight and degree of polymerization, that influences the mechanical properties and thermal properties of polymers.
Molecular structure	Each PE has their specific linear structure that can have branching or crosslink reactions formed during the synthesis which affects resistance, flexibility and solubility of polymer
Reaction kinetics	The fractional parameters obtained can also be correlated with the polymerization efficiency and the presence of faults in the polymer chain
Reaction synthesis	These polymerization methods were validated.

While the predictions with Maxwell fractional model are better than the model of standard fractional order for fluids in 1D, because in fact due to the higher number of parameters [Alves, 2017] I have careful attention because of this. We should not forget that Alves modulated with standard fractional viscoelastic order for fluids in 1D SAOS experimental data points for Dow Affinity PL 1840 and Dow Affinity PL 1880 and it performed well. This is since the normal fractional order viscoelastic for fluids only has one springpot, but the Maxwell fractional model is made up of two springpot in series [Freed et al. 2002].

The fact that PE polymers are recyclable and very slightly damaging to the environment is another significant finding of this work. Thus, our work reveals an intriguing connection between fractional calculus and recyclability, particularly about the management of polymeric materials. Understanding the viscoelastic characteristics of recycled plastic is essential for converting it into LDPE, and these models can be used to improve industrial processes. Fractional viscoelastic analysis makes it possible to determine how recycling materials are affected by multiple cycles. This allows the polymers to be reused without causing harm to the environment. While it's true that items manufactured from recycled plastics may differ from their original qualities, this model ensures that the quality of recycled products is consistent and that processes are adjusted accordingly. Additionally, recycling and viscoelastic modeling may be used to create new sustainable materials with improved physical characteristics for certain uses.

6. Conclusion

In the form of an introduction, a quick review was completed, data was gathered, and a new code was created based on the Normand Mathematica CDF article. Because it was feasible to analyze the relative error for each adjustment and find the relative error to be at its lowest, the results were better than anticipated. Therefore, a relationship between the magnitude order of parameters, the properties of a material, and the precision of the adjustment was discovered. The MFM is valid on a specific interval of behavior, and the

parameters in the SAOS tests for these commercial systems adhere to the thermodynamic restrictions. Ultimately, it was found that Alves' work is more efficient because the MFM model has more parameters than the SFVOF model, but since there are less parameters, this model (gFMM) can match better for recyclability.

7. Literature

Alves, B. M. R. (2017). Modeling Insite ® Technology Ethylene α-olefin resins with Standard FOV fluid in 1D. Journal of King Saud University - Engineering Sciences. https://doi.org/10.1016/j.jksues.2017.01.001

Beena Unni, A., Muringayil Joseph, T. (2024). Enhancing Polymer Sustainability: Eco-Conscious Strategies. Polymers, 16 (13), 1769, https://doi.org/10.3390/polym16131769

Bird, B. R., Armstrong, R. C., & Hassanger, O. (1987). Dynamics of polymeric liquids, Fluid mechanics. Journal of Polymer Science Part C: Polymer Letters, *25*, 649. https://doi.org/10.1002/pol.1987.140251211

Di Paola, M., Pirrotta, A. (2022). Fractional Calculus in Visco-Elasticity. In: Rega, G. (eds) 50+ Years of AIMETA. Springer, Cham. https://doi.org/10.1007/978-3-030-94195-6_16

Doerpinghaus, P. J. (2002). Flow Behavior of Sparsely Branched Flow Behavior of Sparsely Branched Metallocene-Catalyzed Polyethylenes. Faculty of the Virginia Polytechnic Institute and State University.

Exact™ 0201FX Ethylene-based Plastomer Resin. (2012). Retrieved March 30, 2025, from http://www.b2bpolymers.com/TDS/ExxonMobil_Exact_0201FX.pdf

Exxon Mobil NTX 101 (2025), Retrieved March 30, 2025, https://exxonmobilchemical.ides.com/en-US/ds244407/ExxonMobil%E2%84%A2%20NTX%20101.aspx?I=58933&U=0

Freed, A., Diethelm, K., & Luchko, Y. (2002). *Fractional-Order Viscoelasticity (FOV): Constitutive Development Using the Fractional Calculus: First Annual Report*. Retrieved from http://gltrs.nasa.gov

Friedrich, C. (1991). Relaxation and retardation functions of the Maxwell model with fractional derivatives. *Rheologica Acta*, *30*(2), 151–158. https://doi.org/10.1007/BF01134604

Giusti, A., Colombaro. I.,Garra, R., Garrapa, R., Mentrelli,A., (2024). On variable-order fractional linear viscoelasticity, Fractional Calculus and Applied Analysis, v.27, pp. 1564-1578

Jaishankar, a., & McKinley, G. H. (2012). Power-law rheology in the bulk and at the interface: quasi-properties and fractional constitutive equations. *Proceedings of the Royal Society A: Mathematical, Physical and Engineering Sciences*, (1989), 1–21. https://doi.org/10.1098/rspa.2012.0284

Lyondellbasell. (2025). Product detail | LyondellBasell. Retrieved March 30, 2025, from https://www.lyondellbasell.com/en/polymers/p/Petrothene-NA952000/f0c92536-aad4-42f9-9106-2de0d6fefed1

Machado, J. T., Kyriakova, V., & Mainardi, F. (2011). Recent history of fractional calculus. *Communications in Nonlinear Science and Numerical Simulation*, *16*(3), 1140–1153. https://doi.org/http://dx.doi.org/10.1016/j.cnsns.2010.05.027

Macosko, C. (1994). *Rheology: Principles, Measurements and Applications*. *Powder Technology* (Vol. 86). New York: John Wiley & Sons. https://doi.org/10.1016/S0032-5910(96)90008-X

Mainardi,F., Spada,G., Creep Relaxation and viscosity properties for basic fractional models in Rheology,The european Physical Journal, Special Topics, Vol(193), 2011, 133-160

Marsden, J., & Weinstein, A. (1985). *Calculus I* (Second Edi). New York: Springer. Retrieved from http://authors.library.caltech.edu/25030/1/Calc1w.pdf

Normand, M. D., Eisenberg, M., & Peleg, M. (2012). Choosing Initial Parameter Values For Nonlinear Regression. Wolfram Demonstrations Project.

Nutting, P.G., A new general law of deformation, Journal of the franklin Institute, 191 (1921) 679-685

Padilla, P. A., Abreu, H. D., & Mumañ, F. C. (2008). Cálculo Fraccionario, 1–26. Retrieved from http://www.monografias.com/trabajos-pdf/introduccion-calculo-fraccionario/introduccion-calculo-fraccionario.pdf

Ribeiro Alves (2020), Modelizacao viscoelastica fracionária do comportamento em relaxacao da resina polimérica de ABS com software R, RCT - Revista de ciência e técnologia,

Ribeiro Alves (2022), Estudo e afericao da qualidade de ajuste de modelos viscoelásticos em ensaios dinamicos para o polibutadieno com o software Office, RCT - Revista de ciência e técnologia,

Santana, A. M. (2010). *Aplicação das derivadas*. Ji-Paraná. Retrieved from http://www.dmejp.unir.br/menus_arquivos/1787_anderso_marcolino.pdf

Schiessel, H., Metzler, R., Blumen, A., & Nonnenmacher, T. F. (1995). Generalized viscoelastic models: their fractional equations with solutions. *Journal of Physics A: Mathematical and General*, *28*(23), 6567. Retrieved from http://stacks.iop.org/0305-4470/28/i=23/a=012

Schmidt, R.F., Winter H.H., Gradzielski M., 1.Generalized vs. fractional: a comparative analysis of Maxwell models applied to entangled polymer solutions - Soft Matter (RSC Publishing) DOI:10.1039/D4SM00749B

Shitikova, M.V. (2022). Fractional Operator Viscoelastic Models in Dynamic Problems of Mechanics of Solids: A Review. *Mechanics of solids*. **57**, pp. 1–33. https://doi.org/10.3103/S0025654422010022

The fundamental theorem of Calculus. (2010), 3. Retrieved from https://math.berkeley.edu/~ogus/Math_1A/lectures/fundamental.pdf

Vasile, C., & Pascu, M. (2005). *Practical Guide to Polyethylene*. Shawbury: Rapra Technology Limited.

Yang, XJ., Gao, F., Ju, Y. (2022). General Fractional Calculus with Nonsingular Kernels: New Prospective on Viscoelasticity. In: Singh, J., Dutta, H., Kumar, D., Baleanu, D.,

Hristov, J. (eds) Methods of Mathematical Modelling and Computation for Complex Systems. Studies in Systems, Decision and Control, vol 373. Springer, Cham. https://doi.org/10.1007/978-3-030-77169-0_6

Ziegler-Natta Polymerization. (2022). College of Saint Benedict/Saint John's University. https://chem.libretexts.org/@go/page/200848

Ziegler-Natta Polymerizations. (2023). Duke University. https://chem.libretexts.org/@go/page/385633